

# The low-energy spectrum in DAMIC at SNOLAB

Alvaro E. Chavarria\*

Center for Experimental Nuclear Physics and Astrophysics,  
University of Washington, Seattle, United States

\* [chavarri@uw.edu](mailto:chavarri@uw.edu)



14th International Conference on Identification of Dark Matter  
Vienna, Austria, 18-22 July 2022  
doi:[10.21468/SciPostPhysProc.12](https://doi.org/10.21468/SciPostPhysProc.12)

## Abstract

The DAMIC experiment employs large-area, thick charge-coupled devices (CCDs) to search for the interactions of low-mass dark matter particles in the galactic halo with silicon atoms in the CCD target. From 2017 to 2019, DAMIC collected data with a seven-CCD array (40-gram target) installed in the SNOLAB underground laboratory. We report dark-matter search results, including a conspicuous excess of events above the background model below  $200 eV_{ee}$ , whose origin remains unknown. We present details of the published spectral analysis, and update on the deployment of skipper CCDs to perform a more precise measurement by early 2023.



Copyright A. E. Chavarria.

This work is licensed under the Creative Commons  
[Attribution 4.0 International License](https://creativecommons.org/licenses/by/4.0/).

Published by the SciPost Foundation.

Received 04-10-2022

Accepted 24-04-2023

Published 03-07-2023

doi:[10.21468/SciPostPhysProc.12.011](https://doi.org/10.21468/SciPostPhysProc.12.011)



Check for  
updates

## 1 Introduction

The DAMIC experiment at SNOLAB employs the bulk silicon of scientific charge-coupled devices (CCDs) as a target for interactions of particle dark matter (DM) from the galactic halo. The low pixel readout noise of  $1.6 e^-$  R.M.S., combined with extremely low leakage current of a few  $e^-$  per  $\text{mm}^2 \cdot \text{day}$ , provides DAMIC CCDs with sensitivity to the small ionization signals from recoiling electrons or nuclei following the interactions of low-mass DM particles.

## 2 DAMIC at SNOLAB

DAMIC CCDs were developed by Berkeley Lab's Microsystems Laboratory and fabricated by Teledyne DALSA. The devices feature a rectangular array of pixels, each of size  $15 \times 15 \mu\text{m}^2$ , and a fully-depleted active region of  $675 \mu\text{m}$ . Other details of the CCD design and fabrication process can be found in Ref. [1]. Several arrangements of CCDs were deployed in the DAMIC

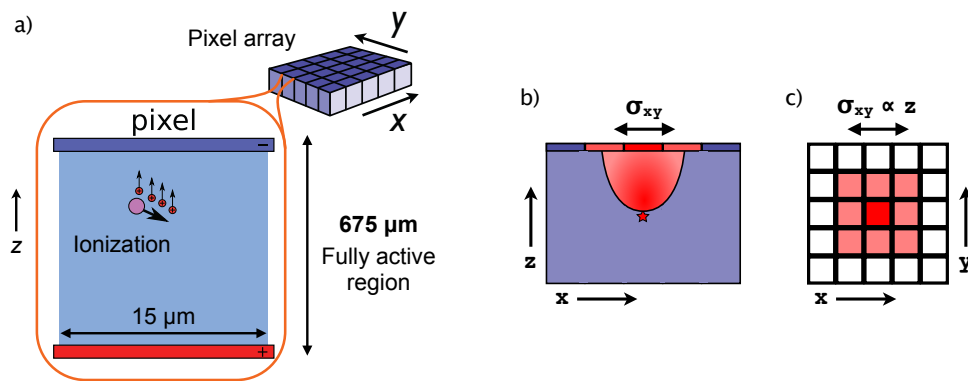


Figure 1: a) Sketch of a low-energy particle ionizing the CCD active region. b) Diffusion of charge as it drifts toward the pixel array. c) The spread of the charge cluster on the pixel array is positively correlated with the depth of the interaction.

cryostat since 2012, with the final installation of seven 16 Mpix CCDs in 2017, for a total silicon target mass of 40 g. Details of the DAMIC setup at SNOLAB are presented in Refs. [2, 3].

DAMIC data consists of images that contain a two-dimensional projection of all charge generated in the active region of the CCDs throughout an image exposure (typically 8 h). Particles generate free charges (e-h pairs) in the CCD active region by ionization (Fig. 1a), with one free e-h pair generated on average for every 3.8 eV of kinetic energy deposited by a recoiling electron. For a recoiling nucleus, the charge yield is lower and non-linear, and was directly calibrated in Ref. [4]. The free charges are then drifted by an electric field toward the pixel array. Since charge diffuses laterally as it drifts, interactions that occur deeper in the CCD bulk lead to more diffuse charge clusters (Fig. 1b). The spread of the charge in the image ( $x$ - $y$  plane) can then be used to reconstruct the depth ( $z$ ) of an interaction in the CCD active region (Fig. 1c). Clustering algorithms are run on DAMIC images to identify clusters of pixels with charge above noise and reconstruct the deposited energy and  $(x, y, z)$  location of particle interactions in the bulk silicon. Details on the CCD response, image cleanup and processing are also presented in Refs. [2, 3].

Dark matter searches in DAMIC are performed by comparing the charge (energy) distributions of individual pixels or pixel clusters against a background model that includes instrumental noise and ionizing backgrounds from natural radioactivity. Ref. [3] provides all details on the construction of the radioactive background model, including the extensive radioassay program of all detector components. The background model was constrained and validated with several independent measurements of radiocontaminants in the detector, e.g., surface/bulk  $^{210}\text{Pb}$  and bulk  $^{32}\text{Si}$ , that were performed with the CCDs themselves by searching for spatio-temporal correlations between decays [5].

The main science results from DAMIC are:

- The first search for DM interactions that produce as little as a one e-h pair in silicon, resulting in the first exclusion limit on the absorption of hidden photons [6] with masses as small as  $1.2 \text{ eV } c^{-2}$  [7].
- Exclusion limits on DM particles [8] with masses as small as  $0.5 \text{ MeV } c^{-2}$  scattering with electrons [9].
- The most sensitive direct search for weakly interacting massive particles (WIMPs) [10–12] with masses in the range  $1\text{--}9 \text{ GeV } c^{-2}$  [13] scattering with silicon nuclei. This result significantly constrains any DM interpretation of the event excess observed by the CDMS-II Si experiment [14], which employed the same nuclear target.

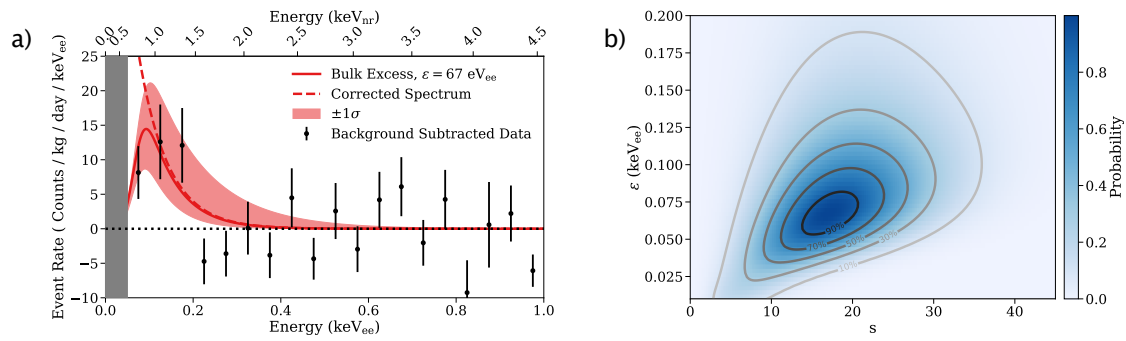


Figure 2: **a)** Energy spectrum of the event excess (red lines) overlaid on the background-subtracted data (markers). Both the best fit spectrum that includes the detector response (solid line) and the spectrum corrected for the detection efficiency (dashed line) are provided. The red shaded region represents the  $1\sigma$  uncertainty from the fit. **b)** Fit uncertainty in the number of excess events over the background model ( $s$ ) and characteristic decay energy ( $\epsilon$ ) of the exponential spectrum. The color axis represents the  $p$ -value from the fit. Figures from Ref. [3].

### 3 Low-energy spectrum

The background model developed for DAMIC’s WIMP search describes the data remarkably well down to 200 eV<sub>ee</sub>. Below this energy, and down to the detector’s 50 eV<sub>ee</sub> threshold, there is a statistically significant excess ( $3.7\sigma$ ) of events whose spatial distribution is consistent with being uniform in the bulk silicon and whose spectrum is well parametrized by a decaying exponential. Figure 2a shows the energy distribution of the excess of events above the background spectrum. The  $p$ -value for the excess as a function of amplitude (number of events in the 11 kg-day exposure) and decay energy of the exponential is shown in Fig. 2b.

Ref. [3] presents a detailed investigation on the origin of the excess. The events are significantly above threshold, and cannot arise from any known sources of instrumental noise (e.g., white readout noise or shot noise from leakage current). Studies were performed on the spatial distribution of the events, and it was concluded that neither the known decaying spectrum from backside events that suffer from partial charge collection or an unknown population of frontside events could explain the excess. Additionally, it was confirmed that besides the excess, there were no other statistically significant deviations from the background model throughout the full energy spectrum. So far, the event excess is consistent with an unknown source of ionization events in the bulk silicon with a rate of a few per kg-day.

### 4 Skipper-CCD Upgrade

To confirm the presence of the excess, and to better understand its origin, novel skipper CCDs were deployed in the DAMIC cryostat at SNOLAB. This activity is carried out in collaboration with the DAMIC-M and SENSEI Collaborations, who provided the skipper CCDs and readout electronics [15]. Figure 3a shows the two 24 Mpix DAMIC-M prototype skipper CCDs (a silicon target of 18 g) being installed in their copper box. The detector upgrade was completed in November 2021 and, following a commissioning period, science-data taking started in March 2022. So far, 3 kg-day of data have been acquired with a total (bulk) radioactive background rate of 9 (6) events per keV<sub>ee</sub>·kg·day, comparable to the previous detector installation. Data taking will continue throughout 2022 with first results expected in early 2023.

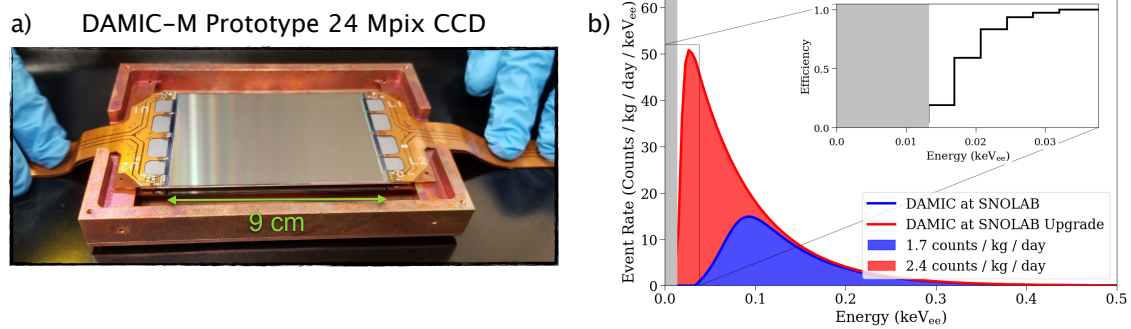


Figure 3: **a)** DAMIC-M 24 Mpix CCDs in their copper box. The bottom CCD is barely visible under the top CCD. **b)** Exponentially decaying spectrum of the excess of events observed in DAMIC at SNOLAB. The blue spectrum is the best-fit from the published analysis [3, 13], while the red spectrum is the expectation for the upgraded detector with skipper CCDs. The measured detection efficiency of the upgraded detector (inset) was used to construct the red spectrum.

Skipper CCDs feature pixel readout noise as low as  $0.05 e^-$ , with the capability of counting with high resolution the number of charges collected in a pixel [16]. The much lower noise will decrease the threshold from  $50 eV_{ee}$  to  $15 eV_{ee}$ , and significantly improve the measurement of the  $x$ - $y$  spread of the clusters for better  $z$  resolution. Figure 3b shows the much larger fraction of the exponentially decaying spectrum that is expected to be observed with skipper CCDs. The skipper-CCD spectrum assumes the noise performance of the detector measured at SNOLAB after deployment, with the detection efficiency provided in the inset.

## 5 Conclusion

Over the past decade, DAMIC pioneered the use of low-noise CCDs in a low-radioactivity underground environment to search for DM. The seven-CCD setup of DAMIC at SNOLAB that operated from 2017 to 2019 accrued the largest exposure with the lowest radioactive background of any CCD DM detector to date. DAMIC published results from several DM searches, placing stringent exclusion limits on the interaction cross sections of DM particles with both electrons and nuclei in silicon atoms. In the latest search for WIMPs, a conspicuous excess of events was observed above the background model below  $200 eV_{ee}$ , whose origin remains unknown. The DAMIC detector at SNOLAB was recently upgraded with ultra-low noise skipper CCDs to clarify the origin of these events.

## Acknowledgements

These proceedings report on the work of the DAMIC Collaboration, currently composed of 38 scientists from 10 institutions around the world. The DAMIC experiment is made possible by SNOLAB and its staff, who provide underground space, logistical and technical services.

## References

- [1] S. Holland et al., *Fully depleted, back-illuminated charge-coupled devices fabricated on high-resistivity silicon*, IEEE Trans. Electron Devices **50**, 225 (2003), doi:[10.1109/TED.2002.806476](https://doi.org/10.1109/TED.2002.806476).
- [2] A. Aguilar-Arevalo et al., *Search for low-mass WIMPs in a 0.6 kg day exposure of the DAMIC experiment at SNOLAB*, Phys. Rev. D **94**, 082006 (2016), doi:[10.1103/PhysRevD.94.082006](https://doi.org/10.1103/PhysRevD.94.082006).
- [3] A. Aguilar-Arevalo et al., *Characterization of the background spectrum in DAMIC at SNO-LAB*, Phys. Rev. D **105**, 062003 (2022), doi:[10.1103/PhysRevD.105.062003](https://doi.org/10.1103/PhysRevD.105.062003).
- [4] A. E. Chavarria et al., *Measurement of the ionization produced by sub-keV silicon nuclear recoils in a CCD dark matter detector*, Phys. Rev. D **94**, 082007 (2016), doi:[10.1103/PhysRevD.94.082007](https://doi.org/10.1103/PhysRevD.94.082007).
- [5] A. Aguilar-Arevalo et al., *Measurement of the bulk radioactive contamination of detector-grade silicon with DAMIC at SNOLAB*, J. Instrum. **16**, P06019 (2021), doi:[10.1088/1748-0221/16/06/P06019](https://doi.org/10.1088/1748-0221/16/06/P06019).
- [6] Y. Hochberg, T. Lin and K. M. Zurek, *Absorption of light dark matter in semiconductors*, Phys. Rev. D **95**, 023013 (2017), doi:[10.1103/PhysRevD.95.023013](https://doi.org/10.1103/PhysRevD.95.023013).
- [7] A. Aguilar-Arevalo et al., *First direct-detection constraints on eV-scale hidden-photon dark matter with DAMIC at SNOLAB*, Phys. Rev. Lett. **118**, 141803 (2017), doi:[10.1103/PhysRevLett.118.141803](https://doi.org/10.1103/PhysRevLett.118.141803).
- [8] R. Essig, M. Fernández-Serra, J. Mardon, A. Soto, T. Volansky and T.-T. Yu, *Direct detection of sub-GeV dark matter with semiconductor targets*, J. High Energy Phys. **05**, 046 (2016), doi:[10.1007/JHEP05\(2016\)046](https://doi.org/10.1007/JHEP05(2016)046).
- [9] A. Aguilar-Arevalo et al., *Constraints on light dark matter particles interacting with electrons from DAMIC at SNOLAB*, Phys. Rev. Lett. **123**, 181802 (2019), doi:[10.1103/PhysRevLett.123.181802](https://doi.org/10.1103/PhysRevLett.123.181802).
- [10] E. Kolb and M. Turner, *The early Universe*, Addison-Wesley, Redwood City, USA, ISBN 9780201116038 (1990), doi:[10.1201/9780429492860](https://doi.org/10.1201/9780429492860).
- [11] K. Griest and M. Kamionkowski, *Supersymmetric dark matter*, Phys. Rep. **333**, 167 (2000), doi:[10.1016/S0370-1573\(00\)00021-1](https://doi.org/10.1016/S0370-1573(00)00021-1).
- [12] K. M. Zurek, *Asymmetric dark matter: Theories, signatures, and constraints*, Phys. Rep. **537**, 91 (2014), doi:[10.1016/j.physrep.2013.12.001](https://doi.org/10.1016/j.physrep.2013.12.001).
- [13] A. Aguilar-Arevalo et al., *Results on low-mass weakly interacting massive particles from an 11 kg d target exposure of DAMIC at SNOLAB*, Phys. Rev. Lett. **125**, 241803 (2020), doi:[10.1103/PhysRevLett.125.241803](https://doi.org/10.1103/PhysRevLett.125.241803).
- [14] R. Agnese et al., *Silicon detector dark matter results from the final exposure of CDMS II*, Phys. Rev. Lett. **111**, 251301 (2013), doi:[10.1103/PhysRevLett.111.251301](https://doi.org/10.1103/PhysRevLett.111.251301).
- [15] G. Canelo et al., *Low threshold acquisition controller for Skipper charge-coupled devices*, J. Astron. Telesc. Instrum. Syst. **7**, 015001 (2021), doi:[10.1117/1.JATIS.7.1.015001](https://doi.org/10.1117/1.JATIS.7.1.015001).
- [16] J. Tiffenberg et al., *Single-electron and single-photon sensitivity with a silicon skipper CCD*, Phys. Rev. Lett. **119**, 131802 (2017), doi:[10.1103/PhysRevLett.119.131802](https://doi.org/10.1103/PhysRevLett.119.131802).